

# Primary Response of Pavement Variation with Construction Variables

Rosnawati Buhari<sup>1, a</sup> and Munzilah Md Rohani<sup>2, b</sup>

<sup>1, 2</sup> Smart Driving Research Centre (SDRC), Faculty of Civil and Environmental Engineering, Universiti Tun Hussein Onn Malaysia, 86400, Johor, Malaysia

[rosna@uthm.edu.my](mailto:rosna@uthm.edu.my), [munzilah@uthm.edu.my](mailto:munzilah@uthm.edu.my)

**Keywords:** influence function, peak influence function, primary response, strain, resilient modulus

**Abstract.** Fatigue and rutting are two major modes of distress of flexible pavements that are typically characterized by the primary response of the pavement and so calculations of the pavement's structural responses should be measured carefully for more accurate predictions of pavement performance. Response to it, this task aims to predict the primary response of the forces using Influence Function and Peak Influence Function Method for several differences top layer pavement thicknesses. In this tasks, both the aforementioned critical responses were highlighted, that are horizontal tensile strain at the bottom of bound layers and the vertical compressive strain on top of the sub-grade layer, that relates to fatigue and rutting damage respectively. The vertical load applied to the surface is uniformly over a circular area, leading to an axial symmetric problem. The pavement structure was modeled as semi-infinite linear elastic system considering three layers; an asphalt surface layer, a granular base layer and semi-infinite sub-grade or soil layer. A multilayer linear elastic approach was used to calculate the response of the pavement structure under uniform contact stress. The simulation results were compared to the results from *BISAR* application. As a finding, the comparison between computed critical strains and output from *BISAR* and a good consensus was reached. The variation of radial and vertical strains at the bottom of asphaltic concrete and on top of the sub-grade layer is matched well and conforms to the capability of the programme that was developed.

## Introduction

In modern pavement design, there are two separate tasks involved. It includes computation of pavement response from the load and the prediction of pavement performance. The critical pavement response used in distress models is calculated in the pavement response models by applying vertical tyre-pavement contact stress to the pavement surface. The contact stress is typically assumed to be distributed evenly over a circular contact area in the vertical direction. At the bottom of the asphalt layer, the horizontal strains are responsible for fatigue. At the top of sub-grade, the vertical strains are the ones that are studied as they will be used to predict pavement rutting.

At constant static load, tyre loading is usually modelled as a circular area with uniform contact pressure loading on to the pavement's layer structure. The structures of road surfaces were traditionally considered to behave as continua, and have utilised the methods of continuum mechanics. In the 1940's, the theory of elastic layered systems was published by Burmister [1]. Layered elastic theory is the tool most often used to calculate flexible pavement response to vehicle loading due to its simplicity. Ullidtz and Huang extended a close-form solution for a two-layered linear elastic half-space problem to a three-layered system [2]-[3]. This linear elastic system allows for the super positioning of multiple wheels for example, the ELSYM computer programme [4]. Kenis then developed

the VESYS program that is also based on the linear elastic response model in which the visco-elastic response was included by the use of the ‘elastic-visco-elastic corresponding principle [5]. This approach was also applied in the NCHRP project [6]. Theoretical calculated stress and strains might also be obtained using software based on layered-elastic theory, for example KENPAVE. This software allowed the use of linear elastic, non-linear, and visco-elastic properties for up to 19 layers and also performed damage analysis. Other than that, other software with the same approach, developed as BISAR 3.0, Elsym5 and Everstress 5.0. An alternative approach that was used for critical response computation is the finite element method. MichPave and 3D Mesh using ABAQUS are examples of software that utilise this method.

## Methodology

In this study, the vertical load applied to the surface is uniformly over a circular area with a diameter measuring 0.3m, leading to an axial symmetric problem. Two dimensions of pavement systems need to be selected: the depth and the radius. Fig. 1 shows the schematics of the pavement layer systems used in this study and details of the pavement structure as well as the pavement materials are listed in Table 1 (Refer [7] for detail of the correlations between the layer parameters ). The coordinate system is chosen as such that  $x$  and  $y$  axes are on the surface of the pavement whilst the  $z$  axis is vertical to the  $x$ - $y$  plane and extends along the depth direction. The radius of the pavement structure is 2m and the depth of 1.5m was applied. In accordance, there are 21 grid points—all of which are equally spaced; 0.1m inside the interval and 16 grid points between 0 to 1.5m inserted within the  $z$  interval.

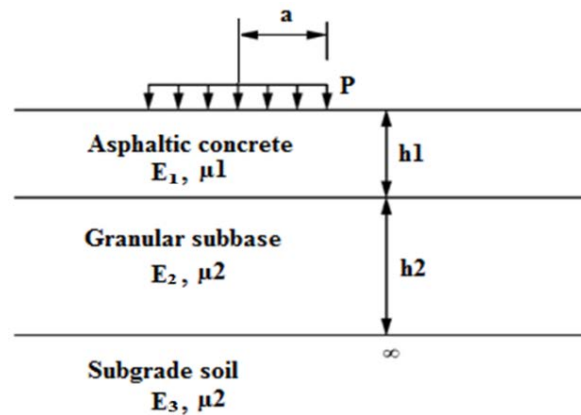


Fig. 1: Pavement structure

The pavement structure were modelled as semi-infinite linear elastic system considering three layers—an asphalt surface layer, a granular base layer and semi-infinite sub-grade or soil layer. For all analyses, the soil  $CBR$  is 5 percent which represents clayey soil. The value of sub-grade elastic modulus,  $E_3$  and Poisson’s ratio for each layer is constant during the analysis. The modulus of sub-grade soil is defined using a correlation between  $CBR$  and sub-grade modulus, ( $E_3 = CBR \times 10$ ). The elastic modulus of the bituminous materials defined at a temperature of 27 Celsius. A multilayer linear elastic approach was used.

Two methods have been used for predicting the primary response; Influence Function and Peak Influence Function Method (Refer [8] for further detail). The vehicle is travelling at constant speed of 20m/s

Table 1 Pavement structure characteristic

Pavement layer	Thickness (mm)	Air void content (%)	Volume of binder, (%)	Modulus (GPa)
Asphaltic layer	200	4	8	$E_1$ { Penetration Index (PI) , AC temperature, AC volume of Void, AC volume of binder & Vehicle speed }
Granular Sub-base	200	-	-	$E_2=0.1E_1$
				$E_2=0.02E_1$
				$E_2=0.01E_1$
Subgrade Soil	infinite	-	-	$E_3$ (CBR- 5%)

### Result and Discussion

Fig. 2 shows the tensile strain at bottom of asphaltic concrete (Strain at 0.2m in the legend) and vertical strain on top of subgrade layer (Strain at 0.4m in the legend). The simulation results have been compared to the results from *BISAR* application. As shown in the figure, a good consensus was reached between computed critical strains and output from *BISAR*. The variation of radial and vertical strains at the bottom of asphaltic concrete and on top of the sub-grade layer is matched well and conforms to the capability of the programme developed to be used in the following tasks.

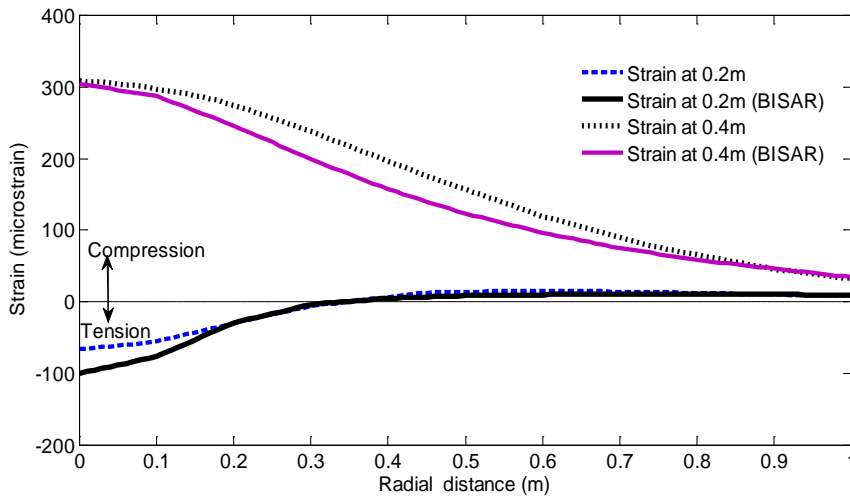


Fig. 2 Comparing predicted radial strain (bottom of asphaltic concrete) and vertical strain (top of sub-grade) as a function of radial distance with result from *BISAR*. The surface vertical load is 30kN

The sensitivity of asphaltic concrete and sub-base layer material elastic modulus was studied. To examine the effect of variations in elastic modulus ratio on the stress and strains generated in the critical points in the pavement, the ratio of the asphalt layer elastic modulus,  $E_1$ , to the granular layer elastic modulus,  $E_2$ , was varied,  $E_1/E_2=10, 50$  and  $100$ . In all conditions the elastic modulus of the asphaltic material is constant. Fig. 3(a) and Fig. 3(b)

displays results of the analyses . In this plots, there are absolute changes in strains due to the corresponding changes of the subbase resilient modulus being estimated. For both strains value, the magnitude is rises when the ratio is higher or subbase condition is less stiffness.

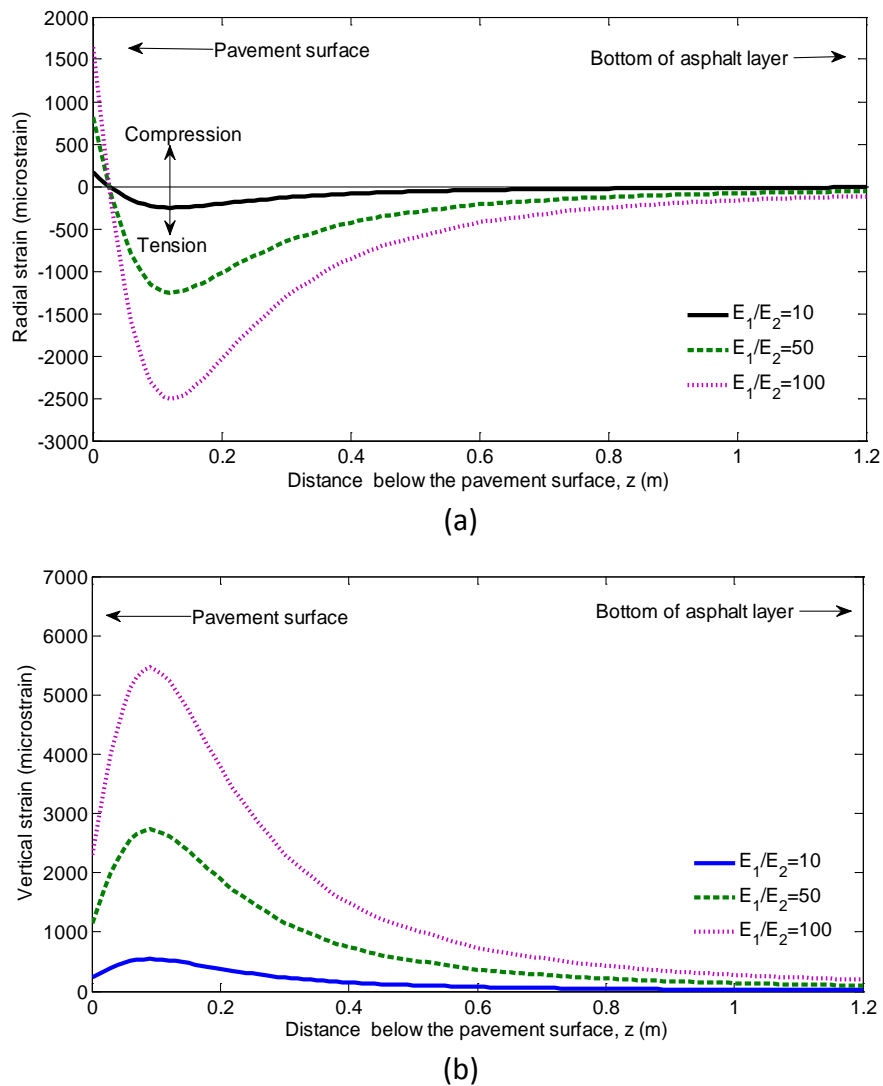
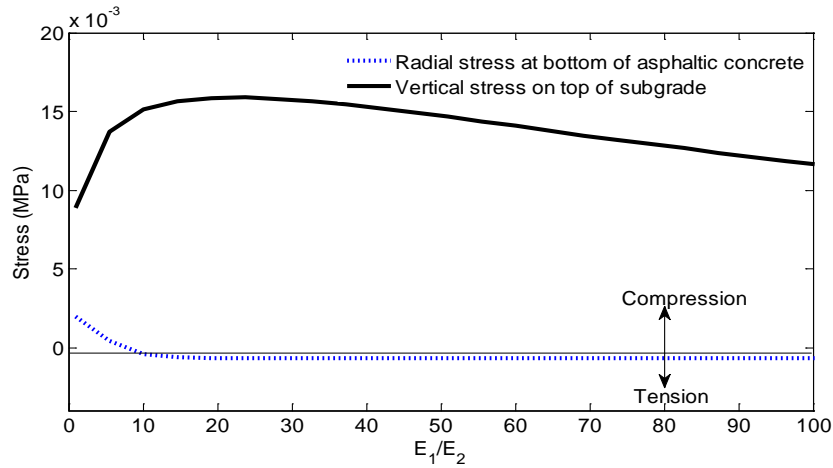


Fig. 3 Radial compression and vertical tension strains as a function of depth using different  $E_1/E_2$ .

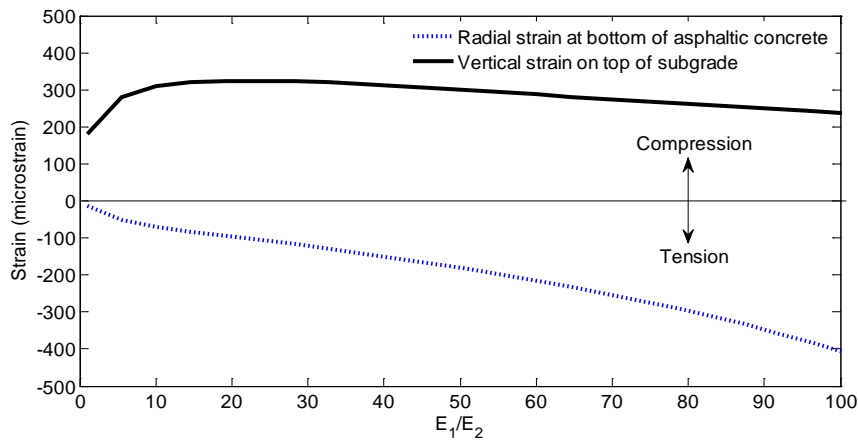
A series of stresses and strains calculated for various  $E_1/E_2$  ratios were performed using the same pavement model. As a results, Fig. 4(a) and Fig 4(b) summarises the peak radial and vertical strains plotted as a function of  $E_1/E_2$  ratio from 1 to 100. It can be seen in this figure that a general trend has been observed for peak radial stress and strain to increase as the  $E_1/E_2$  ratio increase. Besides, for peak vertical stress, it might be divided into two phases. Initially, at lower  $E_1/E_2$  ratio (less than 25) the peak stress increases before it smoothly decreases until  $E_1/E_2$  is 100. The same pattern was observed for vertical strain.

In order to investigate the asphaltic layer thickness' dependency on the critical strain in pavements, a set of asphaltic concrete layer thickness that is, 0.2m, 0.25m and 0.3m, is chosen for analysis. As a result, Fig. 5 is to prove when critical strain is plotted against radial

distance. It can be seen that the general shape of both strain curves are similar, although, as expected, the peak strains for the thicker asphaltic layer have a significantly lower magnitude.



(a) Radial stress (at the bottom of asphaltic concrete) and vertical stress (on top of subgrade) at the centreline of load as a function of different modulus ratios



(b) Radial strains (at the bottom of asphaltic concrete) and vertical strains (on top of subgrade) at the centreline of load as a function of different modulus ratios

Fig. 4 Critical responses as a function of asphaltic concrete modulus to sub-base modulus.

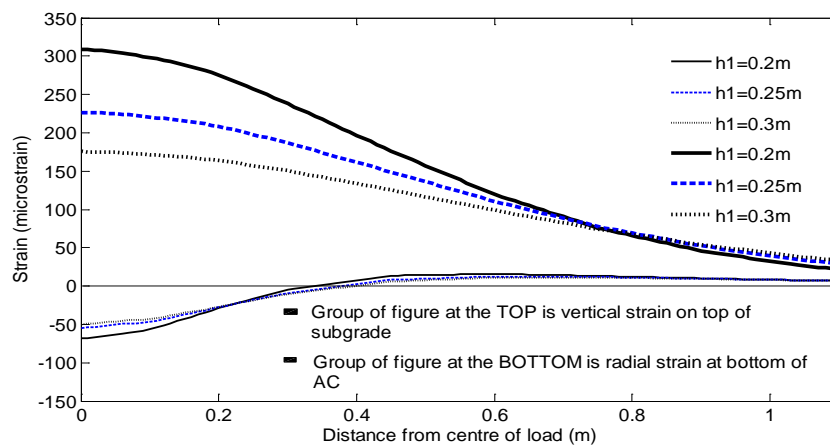


Fig. 5 Radial strains (at bottom of asphaltic concrete) and vertical strains (on top of subgrade) as a function distance for the centre of load using different asphaltic concrete thickness

## Summary

From the analysis, the following can be drawn:

- (1) The elastic modulus of the asphaltic material varies with asphaltic concrete thickness. Increase in the  $E_1/E_2$  was seen to significantly increase critical stresses/strains for fatigue and rutting failure tremendously.
- (2) Stress produced by vehicle loads spread throughout pavements at different weights. The maximum influence function is vertically under the centre of load.
- (3) The compression influence function on top of the subgrade layer is approximately 3.5 times larger than tension influence function at the bottom of the asphaltic layer.

## References

- [1] Burmister, D. M., The general theory of stresses and displacements in layered soil systems 1, 2, 3, J. of Applied Physics, Vol.16, (1945), pp. 296-302.
- [2] Ullidtz, P., Modelling flexible pavement response and performance, (1998), Polyteknisk Forlag, Lyngby, Denmark
- [3] Huang, Y.H., Pavement analysis and Design, Prentice Hall Inc. New Jersey, USA, (1993).
- [4] Monismith, C. L., Inkabi, K., Freeme, C. R., and McLean, D. B., A subsystem to predict rutting in asphalt concrete pavement structures, Proceedings, 4th International Conference on the Structural Design of Asphalt Pavements, Vol. I, Ann Arbor, Michigan, (1977), pp. 529-539.
- [5] Kenis, W. J., Predictive design procedures, a design method for flexible pavements using the VESYS structural subsystem. Proc., 4<sup>th</sup> Int. Conf. on the Structural Design of Asphalt Pavements, ISAP, Lexington, Ky., (1977), pp. 101-147.
- [6] NCHRP, Measuring in situ mechanical properties of pavement subgrade soils, Synthesis of Highway Practice 278, National Cooperative Highway Research Program, TRB, Washington, D.C. USA. (1999).
- [7] Brown, S. F. and Brunton, J. M., An introduction to the analytical design of bituminous pavements, 3<sup>rd</sup> ed., Univ. Of Nottingham, Dept. Of Civil Eng., Nottingham UK. (1992).
- [8] Buhari R., Collop A.C., Pavement Primary Response using Influence Function and Peak Influence Function, Applied Mechanics and Materials, Vols. 256-259, (2013), pp. 1871-1881.